Anal. Bioanal. Electrochem., Vol. 11, No. 1, 2019, 49-58

Analytical & Bioanalytical Electrochemistry

www.abechem.com

Full Paper

Acetanilide Compounds as Corrosion Inhibitors for 304L Stainless Steel in 1 M HCl Solution

El Faiza Larit,[1,*] Mohamed Litim[2] and Hocine Akkari[3]

[1]*Chemical Engineering and Environment Research Laboratory, University 20 August 1955-Skikda, El-Hadaiek Road, BP: 26, 21000 Skikda, Algeria*
[2]*Department of Chemistry, Faculty of Sciences, University 20 August 1955-Skikda, El-Hadaiek Road, BP: 26, 21000 Skikda, Algeria*
[3]*Functional Materials Group, LGMM Laboratory, University 20 August 1955-Skikda, El-Hadaiek Road, BP: 26, 21000 Skikda, Algeria*

*Corresponding Author, Tel.: (+213) 6 64 92 61 98; Fax: (+213) 38 71 55 73
E-Mail: f.larit@univ-skikda.dz

Received: 20 December 2017 / Received in revised form: 11 December 2018 / Accepted: 29 December 2018 / Published online: 31 January 2019

Abstract- The inhibition effect of three acetanilide compounds namely acetanilide (Ac1), *o*-methyl acetanilide (Ac2) and *p*-nitroacetanilide (Ac3) on the corrosion of 304L in 1 M HCl solution was studied by potentiodynamic polarization and electrochemical impedance spectroscopy methods. The results show that compound Ac3 is the best inhibitor and the inhibition efficiency follows the order: Ac3>Ac2>Ac1. Potentiodynamic polarization curves indicated that the inhibitors acted as mixed-type inhibitors. The adsorption of inhibitors on the stainless steel surface obeys to the Langmuir adsorption isotherm and has physisorption mechanism. All techniques employed in this study show the same order of inhibition efficiency.

Keywords- 304L stainless steel, Acetanilide derivatives, Acidic media, Potentiodynamic polarization, EIS

1. INTRODUCTION

The problem of corrosion is prevalent in most industries and it accounts for a huge portion of revenue spent on maintenance due to corrosion damage [1]. Hydrochloric acid solutions are widely used for acid cleaning, industry acid pickling, oil well acidizing and acid descaling [2-4]. Because of aggressive properties of acid solutions on many metals, inhibitors are commonly

used to reduce their corrosive attacks [3]. There are many ways to prevent or reduce metal corrosion such as cathodic or anodic protection, inhibitor application, coating, etc.

The one of the most practical methods for protection versus corrosion damage is using of inhibitors in aggressive media [5]. The ability of corrosion inhibitors to control corrosion is due to the formation of different types of films in different ways, such as adsorption through the formation of sediments or by forming an inactive layer on the metal surface. Several organic inhibitors impeded the corrosion process by forming invisible thin film on the metal surface [6]. However, most of the available organic and inorganic inhibitors may have toxic effects that damage environment and underground resources [7].

Most of the well-known acid inhibitors are organic compounds containing nitrogen, sulphur, oxygen and functional groups through which they are adsorbed on metal surface [8,9]. A large number of organic compounds were studied as corrosion inhibitors, unfortunately most of the organic inhibitors used are very expensive and health hazards.

Their toxic properties limit their field of application [10]. These compounds have the ability to accept or donate electrons in order to be adsorbed on metallic surfaces by electrostatic interactions, i.e, interaction between the free electron pair of corrosion inhibitor containing N, S, O and P atoms and metal**.** Furthermore, their protective properties can be identified as inductive (I), medial (M) and stereotactic effects of substitutions on an acetanilide loop [11].

The importance of alternative electron donation groups, such as the methyl-CH_3 group, which has the effect of I^+ and M^+, on the negative charge on the aromatic ring, and will enhance interaction with the surface of the metal. Also, we do not forget that some autocratic groups that have the ability to pull the electron, such as Nitro-NO_2 groups that have both I-and -M effect, are working to increase the positive charge of the center of the interaction and weaken the interaction [12].

Previous studies have shown that heterocyclic compounds act as effective inhibitors for metallic corrosion. Their effectiveness is based on the presence of heteroatoms, π-electrons, non-bonding electrons and aromatic rings [13]

In recent year the development of the novel corrosion inhibitors like drugs seems to be ideal candidates to replace traditional toxic corrosion inhibitors. Medical drugs can be successfully used as corrosion inhibitors for metals in various media [14,15,16].

Acetanilide is a derivative of aniline, where one of the hydrogens on the nitrogen atom has been replaced with an acetyl group. Acetanilide has a wide variety of uses and is a useful building block in organic synthesis. We are going to be exploring acetanilide in terms of its structure and how it is synthesized, a few important applications it finds use in, and finally we will briefly mention a health concern associated with its use. It is easy to synthesize and readily available. Their ring moiety constitutes a part of the chemical structures of analgesic drugs and other pharmaceuticals [17,18].

As we mentioned previously, acetanilide finds a wide variety of uses in several applications. It has been used in the manufacture of colored dyes for fabrics and textiles, as a reagent in the production of rubber, and as a hydrogen peroxide decomposition inhibitor. Probably what it's best known for however is its role in the pharmaceutical field. In the late 1800s, acetanilide was found to possess painkilling properties, and was introduced as an analgesic under the name Antifebrin.

Among the many substances that have been recommended in turn, to combat fever (..., acetanilide, ...) three have remained in common use: Widal, Lemierre, Abramids [19].

In the present work, three acetanilide compounds, namely acetanilide (Ac1), *o*-methylacetanilide (Ac2) and *p*-nitroacetanilide (Ac3) were used to investigate their inhibition behavior for 304L stainless steel in 1 M HCl solution using Tafel polarization curves and electrochemical impedance spectroscopy (EIS).

2. MATERIALS AND EXPERIMENTAL METHODS

304L stainless steel specimen having the following nominal composition (wt%) are used: Cr 18-20; Ni 8-12; Mn 2; P 0.045; C 0.03; Si 0.75; S 0.03 and Fe balance. The specimens with dimension of 1 cm×1 cm with an exposed area of 1 cm^2 (the rest is covered with yellow resin) were used in both polarization and EIS experimental methods.

Prior to all measurements, the specimens were mechanically abraded with series of emery papers up to 2400, then washed thoroughly with distilled water, degreased with acetone and dried at room temperature. The corrosive media, 1 M HCl solution was prepared by dilution of 37% AR grade HCl with double distilled water. The concentration range of the acetanilide derivatives employed was 5, 10, 15 and 20 ppm. The acetanilide compounds were purchased from Sigma reagent-Aldrich reagent supplier.

Table 1 shows the molecular structure of the acetanilide compounds which have been labelled Ac1, Ac2 and Ac3. These compounds are insoluble in water however they are soluble in Ethanol (EtOH). Accordingly, a stock solution was prepared in EtOH and then diluted to required concentration (5-20 ppm). However, the same quantity of EtOH was added to the blank solution (1 M HCl) to correct its effect.

The electrochemical measurements were carried out using a potentiostat (Radiometer Analytical PGZ 301) piloted by Voltamaster 4 software. The cell consists of three electrodes namely, the working electrode (304L), counter electrode (coiled platinum wire; 99.99% pure, OD=0.5 mm, surface area=4.7 cm^2) and reference electrode (Ag/AgCl; Radiometer Analytical XR300).

We used a 1 hour immersion time to allow the installation of open circuit potential before any electrochemical measurements. We conducted each experiment three times and an average value was reported. All potentials have been reported with respect to the reference pole. For Tafel measurements, and the current potential curves were recorded at a scan rate of 0.5 mV/s

The corrosion parameters such as corrosion potential (E_{corr}), corrosion current (i_{corr}) and cathodic Tafel slope (β_c) were determined by processing with Voltamaster 4 software.

Table 1. Acetanilide derivatives studied as corrosion inhibitors for 304L stainless steel in 1 M HCl solution

Inhibitor	**Structure**	**Abbreviation**
Acetanilide	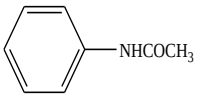	Ac1
Ortho-méthylacétanilide	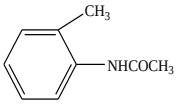	Ac2
Para-nitroacétanilide	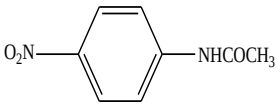	Ac3

Electrochemical impedance measurements were carried out by using AC signal with an amplitude of 10 mV at open circuit potential (OCP) in the frequency range from 100 kHz to1 mHz. The impedance data were fitted to most appropriate equivalent circuit by using Z_{view} software.

3. RESULTS AND DISCUSSION

3.1. Polarization studies

Polarization profiles for 304L steel in 1 M HCl in the presence of different concentration of Ac1, Ac2 and Ac3 at 25 °C are presented in Fig. 1.

The values of associated corrosion electrochemical parameters, i.e., corrosion potential (E_{corr}), corrosion current density (i_{corr}), cathodic Tafel slope (β_c) derived from these curves by extrapolation, as well as the percentage inhibition efficiency (IE%) are listed in Table 1.

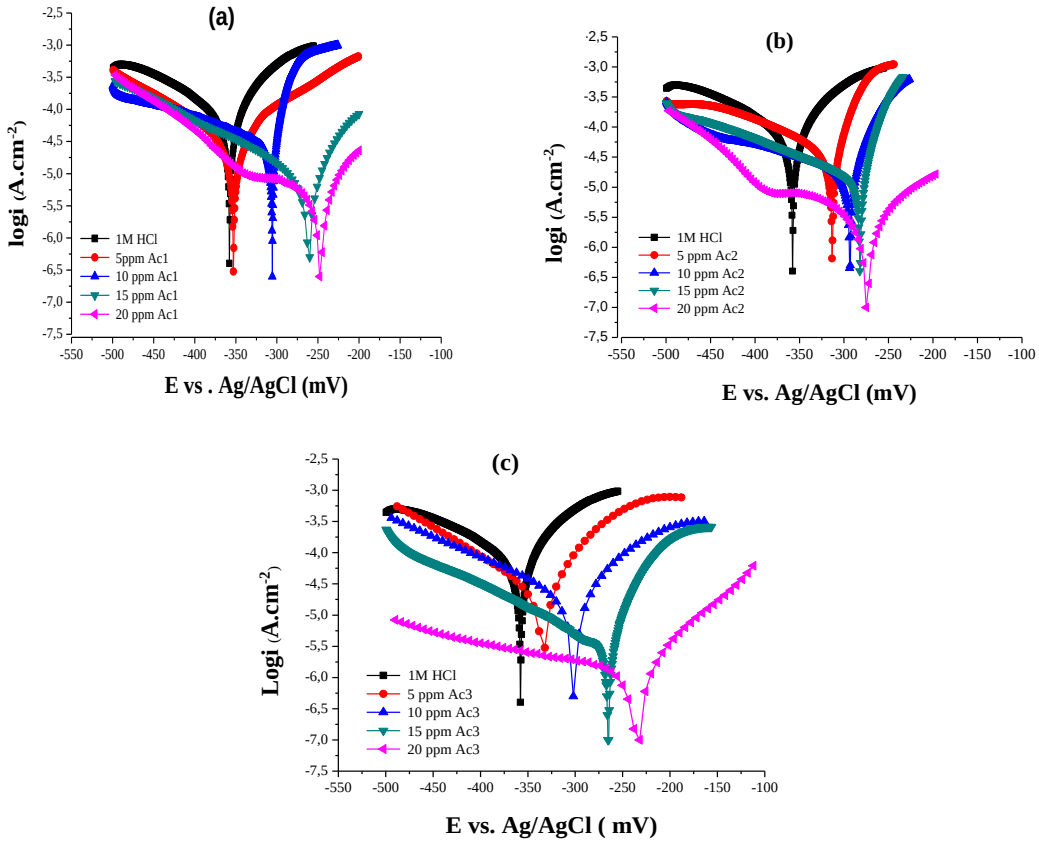

Fig. 1. Polarization curves for 304 SS in 1 M HCl in the absence and presence of Ac1, Ac2 (b) and Ac3 (c) at 25 °C

Table 2. Electrochemical parameters obtained from the polarization curves for various concentration of inhibitors at 25 °C

Inhibitor	C_{inh} (ppm)	E_{corr} (mV)	I_{corr} (A/cm^2)	R_P (Ω.cm^2)	-ß$_c$ (mV)	IE (%)
Ac1	0	-360,0	86,75	209,27	150	-
	5	-354.0	38.80	511.74	154	55.27
	10	-306.0	24.60	679.80	158	71.64
	15	-273.4	10.46	1980.0	159	87.94
	20	-253.9	3.76	4420.0	151	95.66
Ac2	5	-315.2	42.70	480.00	152	50.80
	10	-295.4	16.57	628.90	148	80.90
	15	-290.1	10.30	875.10	153	88.12
	20	-284.1	3.45	6880.0	159	96.02
Ac3	5	-355.0	30.15	513.30	148	65.24
	10	-327.2	20.77	882.10	155	76.05
	15	-266.4	5.51	2730.0	143	93.75
	20	-244.5	3.20	3940.0	157	96.31

The IE% is defined by the following equation [20]:

$$IE\% = \frac{i^0_{corr} + i_{corr}}{i^0_{corr}}.100 \quad (1)$$

where i^0_{corr} and i_{corr} are the corrosion current density values without and with inhibitor, respectively.

From the results in Table 2, it can be observed that the values of corrosion current density (i_{corr}) of stainless steel in the inhibitor-containing solutions were lower than those of stainless steel in the inhibitor-free solution.

From Fig. 1, it is clear that both anodic metal dissolution and cathodic reduction reactions were inhibited when the acetanilide compounds were added to the acid solution and this inhibition was more pronounced with increasing inhibitor concentration.

The presence of acetanilide compounds in HCl solution resulted in the shift of corrosion potential towards more noble direction in comparison with that obtained in the absence of inhibitor. These results show that the addition of these compounds to HCl solutions reduces the anodic dissolution of stainless steel and also delays the cathodic hydrogen evolution reaction. It is also observed that the addition of inhibitors shifted slightly the E_{corr} toward the positive direction with reference to the blank solution. According to conclusion drawn by previous literature data [21,22], if the displacement value in the positive direction of corrosion is greater than 85 mV with respect to the corrosion potential of the empty solution, the inhibitor can be considered as an anode type

The study of cathodic polarization curves leads to the emergence of parallel tributary lines with cathodic cascades (βc). This indicates that the addition of the inhibitor to the aggressive solution does not alter the mechanism of proton reduction and is controlled.

The inhibitor is first adsorbed onto metal surface and then impeded by merely blocking the active sites of steel surface. Thus, the surface area available for H^+ ions decreased, while the actual reaction mechanism remains unaffected [23]. The values of i_{corr} decrease with the increase of the acetanilide derivatives concentrations. We note that the corrosion current densities were more significantly reduced in the presence of Ac3 and became only 3.20 A/cm^2 at 20 ppm. The best efficiency 96.31% is obtained at 20 ppm Ac3 [24]. It is clear that the addition of the acetanilide derivatives leads to decrease of the current density and the inhibition efficiency increases with inhibitor concentration. This can be explained by the adsorption of the compounds organic on the metal surface. Thus, the high inhibition efficiency for acetanilide derivatives can be attributed to the presence of electron donor group ($RR'NCOCH_3$) in their structure **[**25].

3.2. EIS studies

The electrochemical impedance spectra for steel in 1 M HCl in the presence of different concentration of inhibitors at 25 °C are presented as Nyquist plot in Fig. 2. An equivalent circuit model proposed to fit EIS data is shown in Fig. 3.

As can be seen in Fig. 2, the Nyquist plots contain a depressed semi-circle, with the center below the real X-axis, which diameter increases by increasing the inhibitor concentration, indicating that the corrosion is mainly a charge transfer process [26].

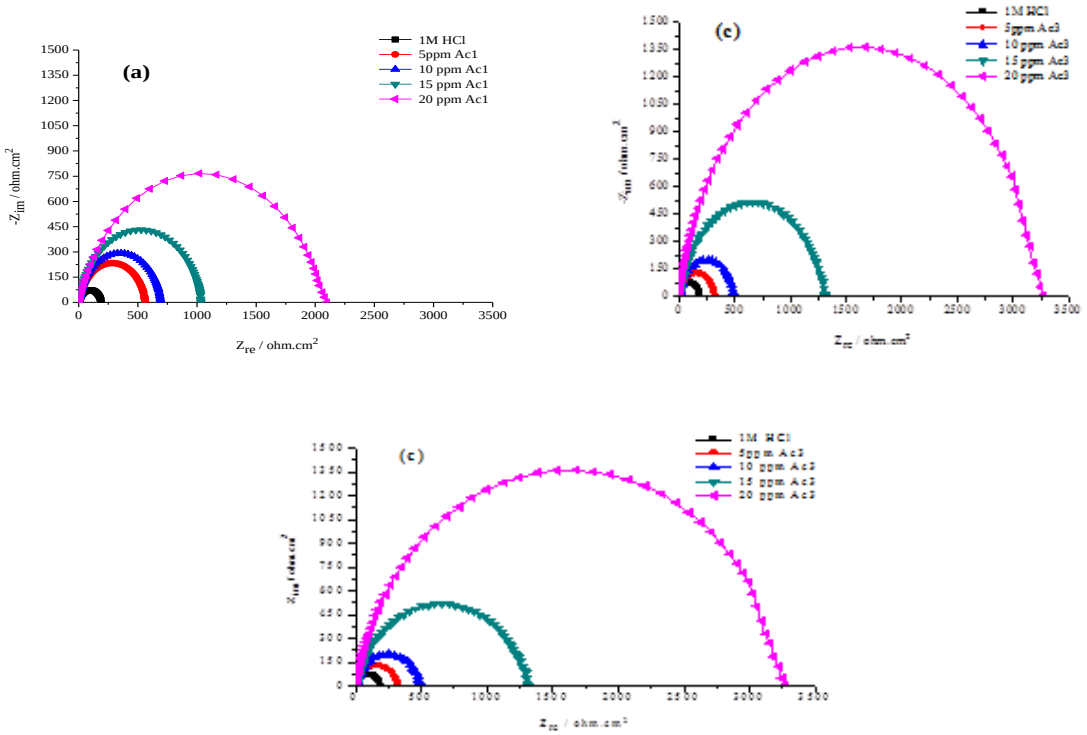

Fig. 2. Nyquist plots for 304L in 1 M HCl solution in the absence and presence of Ac1, Ac2 and Ac3 at 25 °C

The extracted impedance parameters analyzed by EIS analyzer software, are listed in Table 3. The inhibitor efficiency can also be estimated by charge transfer resistance according to the following formula [27,28]:

$$IE\% = \frac{R_{ct} + R_{ct}^{0}}{Y_0}.100 \qquad (2)$$

where R^0_{ct} and R_{ct} are the charge transfer resistance values in the absence and presence of inhibitor, respectively.

Table 3. Impedance parameters for 304L stainless steel in 1 M HCl solution in the absence and presence of acetanilide compounds with different concentrations at 25 °C

Inhibitor	C_{inh} (ppm)	R_s ($\Omega.cm^2$)	CPE		R_{ct} ($\Omega.cm^2$)	C_{dl} ($\mu F.cm^{-2}$)	IE (%)
			Y_0 ($\mu F.cm^{-2}$)	n			
	0	2.91	350	0.84	189.4	199.1	-
Ac1	5	2.20	243	0.89	591.5	160.2	67.9
	10	2.19	207	0.87	696.4	140.8	72.8
	15	2.50	195	0.88	1095	116 .3	82.7
	20	2.40	170	0.85	2092	99.80	91.0
Ac2	5	2.40	255	0.85	399.5	159.2	52.6
	10	3.10	198	0.86	695.6	135.3	72.7
	15	3.20	176	0.88	1157	98.30	83.6
	20	2.79	146	0.89	3098	91.70	93.9
Ac3	5	3.00	255	0.86	324.7	155.8	41.6
	10	2.52	218	0.87	492.8	130.5	61.5
	15	2.55	175	0.85	1303	102.3	85.4
	20	2.32	107	0.88	3262	87.2	94.2

Randles equivalent circuit model (Fig. 3), which is a parallel combination of the charge transfer resistance (R_{ct}) and the constant phase element (CPE), both (R_{ct}) and (CPE) are in series with the solution resistance (R_s). The semicircles are observed to be depressed into the real axis of the Nyquist plot as a result of the roughness of the metal surface. This behaviour has been described and discussed by other researchers [29]. It is modeled by a power-law-dependent capacity term known as the constant phase element (CPE). This kind of phenomenon is known as the ‘‘dispersing effect” [30,31].

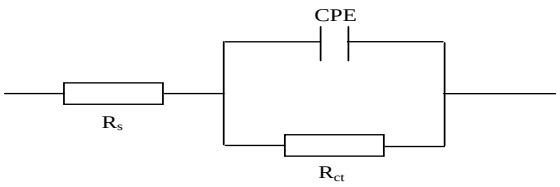

Fig. 3. Equivalent circuit model used to fit the EIS results

Bearing in mind that double-layer resistance does not act as an ideal condenser in the presence of a dispersion effect, the CPE is used as an alternative to the capacitor in Fig. 4 to more precisely match the impedance behavior of the electric double layer. Fixed phase elements have been used extensively to calculate deviations caused by surface roughness. CPE resistance is given by:

$$Z_{CPE} = \frac{1}{Y_0} \times \frac{1}{(j\omega)^n} \quad (3)$$

Where Y_0 is the magnitude of the CPE, n the CPE exponent (phase shift), $\omega = 2\pi f$, the angular frequency where *f* is the AC frequency, and j is the imaginary unit. Depending on the value of the exponent n, CPE may be a resistance, R (n=0); a capacitance, C (n=1); a Warburg impedance, W (n=0.5) or an inductance, L (n=-1) [32].

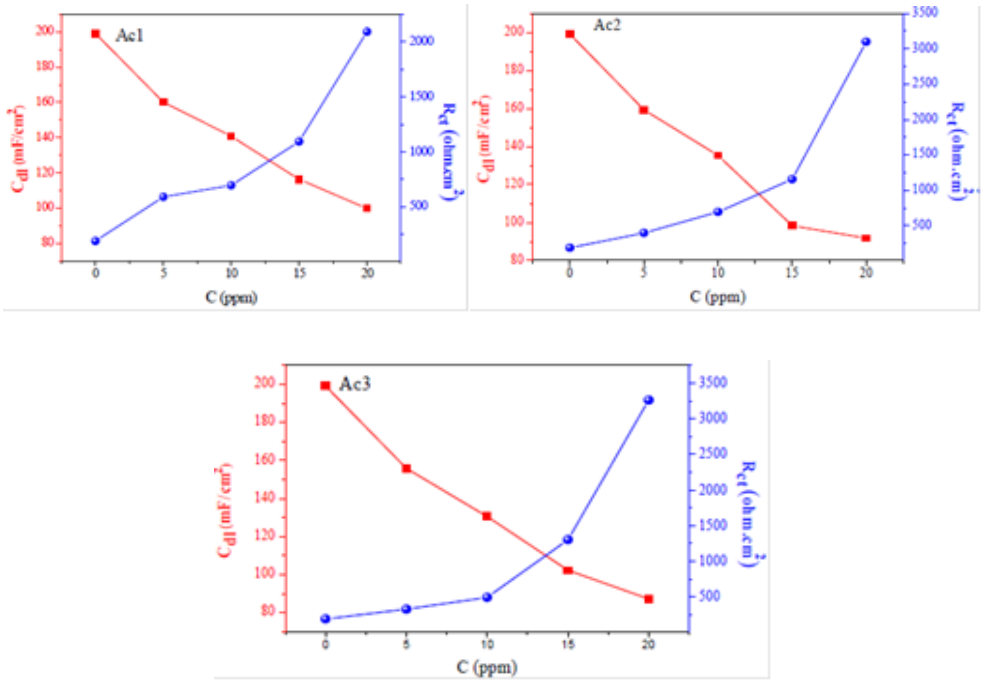

■: C_{dl} and ●: R_{ct}

Fig. 4. Evolution of charge transfer resistance and double-layer capacitance as a function of acetanilide derivatives concentrations

From Table 2, one may notice that the R_{ct} values increase while the C_{dl} values decrease with increasing inhibitor concentration. This result indicates a decrease in the active surface area caused by the adsorption of the inhibitor on the stainless steel surface, and it suggests that the corrosion process became hindered; this hypothesis is corroborated with the anodic and cathodic polarization curves and the corrosion potential values. Furthermore, C_{dl} decreases with increasing of the inhibitor concentration (Fig. 4).

The double-layer capacitance (C_{dl}) was calculated from the following equation:

$$C_{dl} = \frac{1}{2\pi f \max R_{ct}} \tag{4}$$

Where f_{max} is the frequency at which the imaginary component of the impedance is maximal.

3.3. Adsorption isotherms

Adsorption isotherms provide information about the interaction of the adsorbed molecules with the metal surface [33,34].

The adsorption of an organic adsorbate at metal–solution interface can be presented as a substitution adsorption process between the organic molecules in aqueous solution, ($Org_{(sol)}$), and the water molecules on metallic surface, ($H_2O_{(ads)}$) [35]:

$$Org_{(sol)} + xH_2O_{(ads)} \Leftrightarrow Org_{(ads)} + xH_2O_{(sol)} \quad (5)$$

Where $Org_{(sol)}$ and $Org_{(ads)}$ are the organic species dissolved in the aqueous solution and adsorbed onto the metallic surface, respectively, $H_2O_{(ads)}$ is the water molecule adsorbed on the metallic surface and x is the size ratio representing the number of water molecules replaced by one organic adsorbate.

Various relations of isotherms were tested to determine the adsorption mechanism and its parameters as the equilibrium constant K_{ads} and standard free energy, ΔG°_{ads} of adsorption process. The Langmuir model fitted best the straight line obtained (Fig. 5).

According to this isotherm, the surface coverage θ is related to the equilibrium adsorption constant K_{ads} and the concentration of the inhibitor [36,37].

$$\frac{C_{inh}}{\theta} = \frac{1}{K_{ads}} + C_{inh} \quad (6)$$

Where C_{inh} is the inhibitor concentration, K_{ads} is the equilibrium adsorption constant and θ is the surface coverage. The K_{ads} values can be calculated from the intercept lines on the C/θ axis. This is related to the standard free energy of adsorption (ΔG°_{ads}) according to the following equation [38-41]:θ

$$\Delta G^{0}_{ads} = -RT \ln(-55.5K_{ads}) \quad (7)$$

Where R is the gas constant and T is the absolute temperature. The constant value of 55.5 is the concentration of water in solution in mole/dm^3. The values of K_{ads} and ΔG°_{ads} for Ac1, Ac2 and Ac3 are given in Table 4.

The negative sign of ΔG°_{ads} indicates that the inhibitors are spontaneously adsorbed onto the metal surface [34-38]. Generally, the magnitude of ΔG°_{ads} around-20 kJ/mol or less negative is assumed for electrostatic interactions existence between inhibitor and the charged metal surface (i.e., physisorption). Those around -40 kJ/mol or more negative are indicating of charge sharing or transferring from organic species to the metal surface to form a coordinate type of metal (i.e., chemisorption) [39,40-42].

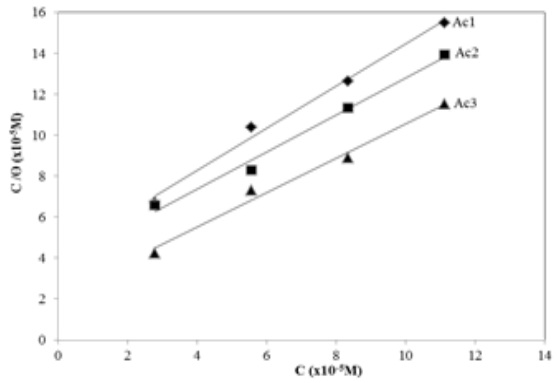

Fig. 5. Langmuir adsorption isotherms for the investigated inhibitors in 1 M HCl at 25 °C

Table 4. Adsorption parameters calculated from the Langmuir adsorption isotherms of acetanilide compounds on 304L stainless steel surface in 1 M HCl solution

Inhibitor	$K_{ads}.10^4$ (M^{-1})	- ΔG^o_{ads}(KJ/mol)	slope	Intercept	R^2
Ac1	2.50	35.02	0.78	4.01	0.991
Ac2	2.66	35.20	0.75	3.75	0.988
Ac3	4.66	36.56	0.84	2.14	0.987

Regarding the present work, the calculated ΔG°_{ads} values for Ac1, Ac2 and Ac3 show that adsorption is a physisorption type between the inhibitors and charged metal surface. The higher values of K_{ads} and ΔG°_{ads} refer to higher adsorption and higher inhibiting effect.

In order to understand the difference between acetanilide derivatives; one can observe the addition of methyl group to acetanilide ring particularly at position 2 leads to the increase in electron density over that of acetanilide ring and the adsorption onto metal surfaces through nitrogen atoms is hindered. Thus *p*-nitroacetanilide is a better inhibitor than *o*-methylacetanilide which is, in fact, experimentally observed.

4. CONCLUSION

All the studied acetanilide compounds showed good inhibition properties for the corrosion of 304 SS in 1 M HCl solutions. The obtained inhibition efficiency of acetanilide compounds from EIS, and polarization curves have the same trend. Inhibition efficiencies are related to concentration, and chemical structure of acetanilide compounds. Tafel polarization curves and EIS results indicate that acetanilide compounds act as good mixed type inhibitors for 304L in 1 M HCl solution. The inhibition efficiency increases with increasing the concentration of the inhibitors.

The negative values of ΔG°_{ads} indicate that the adsorption of the derivatives of acetanilide is a spontaneous process and an adsorption mechanism is typical of physisorption mechanism.

Theoretical adsorption isotherms and thermodynamic calculus shows that the adsorption of inhibitors obeys to the Langmuir adsorption isotherm. All techniques employed in this study show the same order of inhibition efficiency: Ac3>Ac2>Ac1.

REFERENCES

[1] R. T. Loto, and O. Olowoyo, SAJCE 26 (2018) 35.
[2] L. F. Li, P. Caenen, and J. P. Celis, Corros. Sci. 50 (2008) 804.
[3] P. B. Raja, M. Ismail, S. Ghoreishiamiri, J. Mirza, M. C. Ismail, S. Kakooei, and A. Abdul Rahim, Chem. Eng. Commun. 203 (2016) 1145.
[4] M. Finšgar, and J. Jackson, Corros. Sci. 86 (2014) 17.
[5] A. S. Fouda, S. M. Rashwan, S. M. Shaban, H. E. Ibrahim, and M. F. Elbhrawya, Egypt. J. Pet. 27 (2018) 295.
[6] S. B Al-Baghdad, F. G. Hashim, A. Q. Salam, T. K. Abed, T. S. Gaaz, A. A. Al-Amiery, A. Amir H. Kadhum, K. S. Reda, and W. K. Ahmed, Results Phys. 8 (2018) 1178.
[7] Z. Mohammadi, and M. Rahsepar, J. Alloy. Compd. 770 (2019) 669.
[8] S. A. Ali, H. A. Al-Muallem, S. U. Rahman, and M. T. Saeed, Corros. Sci. 50 (2008) 3070.
[9] A. Chetouani, B. Hammouti, T. Benhadda, and M. Daoudi, Appl. Surf. Sci. 249 (2005) 375.
[10] A. S. Fouda, S. A. Abd El-Maksoud, and H. M. S. Badawy, J. Appli. Chem. 6 (2017) 138
[11] T. Yanardag, S. Özbay, S. Dinçer, and A. A. Aksut, Asian. J. Chem. 24 (2012) 47.
[12] G. Gökhan, Corros. Sci. 53 (2011) 3873.
[13] C. Verma, A. A. Sorourc, E. E. Ebensoa, and M. A. Quraishic, Results Phys. 10 (2018) 504.
[14] I. Rotaru, S. Varvara, L. Gaina and L. M. Muresan, Appl. Surf. Sci. 321 (2014) 188.
[15] M. N. El-Haddad, RSC Adv. 6 (2016) 57844.
[16] P. Geethamani, and P. K. Kasthuri, Cogent Chem. 1 (2015) 1.
[17] C. R. Moyes, R. Berger, S. D. Goble, B. Harper, D. M. Shen, L. Wang , A. Bansal, P. N. Brown, A. S. Chen, K. H. Dingley, J. Di Salvo , A. Fitzmaurice, L. N. Gichuru, A. L. Hurley, N. Jochnowitz , R. R. Miller, S. Mistry, H. Nagabukuro , G. M. Salituro, A. Sanfiz, A. S. Stevenson, K. Villa, B. Zamlynny, M. Struthers, A. E. Weber, and S. D. Edmondson, J. Med. Chem. 57 (2014) 1437.
[18] D. Lednicer, and L. Mitscher, The Organic Chemistry of Drug Synthesis, Wiley, New York 310 (1977) 767.
[19] F. Widal, P. J. Teissier, and G. H. Roger, Nouveau traité de médecine, fasc, 3 (1920-1924) pp. 226
[20] H. Zarrok, R. Saddik, H. Oudda, B. Hammouti, A. El Midaoui, A. Zarrouk, N. Benchat, and M. Ebn Touhami, Der Pharma Chem. 3 (2011) 272.

[21] E.S. Ferreira, C. Giancomelli, F.C. Giacomelli, and A. Spinelli. Mater. Chem. Phys. 83 (2004) 129.
[22] O. L. Riggsjr, Corrosion inhibitor, 2nd ed. Nathan, Houston (1973).
[23] R. Solmaz, G. Kardas, B. Yazıcı, and M. Erbil, Coll. Surfaces A 312 (2008) 7.
[24] M. Benabdellah, R. Touzan, A. Aouniti, A.S. Dafali, S. El Kadiri, B. Hammouti, and M. Benkaddour, Mater. Chem. Phys. 105 (2007) 373.
[25] M. El Faydy, M. Galai, R. Touir, A. El Assyry, M. Ebn Touhami, B. Benali, B. Lakhrissi, and A. Zarrouk, J. Mater. Environ. Sci. 7 (2016) 1406.
[26] F. Bentiss, M. Lagrenee, M. Traisnel, and J.C. Hornez, Corros. Sci. 41 (1999) 789.
[27] I. Ahamad, R. Prasad, and M. A. Quraishi, Corros. Sci. 52 (2010) 3033.
[28] J. Aljourani, K. Raeissi, and M. A. Golozar, Corros. Sci. 51 (2009) 1836.
[29] Q. Qu, Sh. Jiang, W. Bai, and L. Li, Electrochim. Acta 52 (2007) 6811.
[30] A. Igual Munoz, J. Garcia Anton, J. L. Guinon, and V. Perez Herranz, Corros. Sci. 49 (2007) 3200.
[31] X. Liu, Shenhao Chen, H. Ma, G. Liu, and L. Shen, Appl. Surf. Sci. 253 (2006) 814.
[32] C. Jeyaprabha, S. Sathiyanarayanan, and G. Venkatachari, Appl. Surf. Sci. 253 (2006) 432.
[33] A. Ehteram. Noor, and H. Aisha Al-Moubaraki, Mater. Chem. Phys. 110 (2008) 145.
[34] G. Avci, Coll. Surfaces. A 317 (2008) 730.
[35] E. Naderi, A. H. Jafari, M. Ehteshamzadeh, and M. G. Hosseini, Mater. Chem. Phys. 115 (2009) 852.
[36] M. Scendo, Corros. Sci, 47 (2005) 2778.
[37] X. L. Wang, Y. Wan, Y. Zeng, and Y. Gu, Int. Electrochem. Sci. 7 (2012) 2403.
[38] H. Amar, A. Tounsi, A. Makayssi, A. Derja, J. Benzakour, and A. Outzourhit, Corros. Sci. 49 (2007) 2936.
[39] O. Benali, L. Larabi, M. Traisnel, L. Gengembra, and Y. Harek, Appl. Surf. Sci. 253 (2007) 6130.
[40] F. Bentiss, M. Lebrini, and M. Lagrenee, Corros. Sci. 47 (2005) 2915.
[41] F. Xu, J. Duan, S. Zhang, and Hou. Baorong, Mat. Lett. 62 (2008) 4072.
[42] E. Machnikova, K. H. Whitmire, and N. Hackerman, Electrochem. Acta 53 (2008) 6024.